



System Level Design Simulation to Predict Passive Safety Performance for CFRP Automotive Structures

2013-01-0663

Published
04/08/2013

Juergen Lescheticky
BMW Group

Graham Barnes
Engenuity Limited

Marc Schrank
Dassault Systemes Simulia Corp.

Copyright © 2013 SAE International

doi:10.4271/2013-01-0663

ABSTRACT

Despite increasingly stringent crash requirements, the body structures of future mainstream production cars need to get lighter. Carbon fiber reinforced polymer (CFRP) composites with a density 1/5th of steel and very high specific energy absorption represent a material technology where substantial mass can be saved when compared to traditional steel applications. BMW have addressed the demanding challenges of producing several hundred composite Body-in-White (BIW) assemblies a day and are committed to significant adoption of composites in future vehicle platforms, as demonstrated in the upcoming i3 and i8 models. A next step to further integrate composites into passenger cars is for primary structural members, which also perform critical roles in passive safety by absorbing large amounts of energy during a crash event.

In order to move forward the integration of CFRP materials in primary structures, the same high level of confidence in passive safety design simulations achieved by BMW for metallic structures needs to be achieved with composites designs. Following encouraging results from early component level studies using the CZone extension for Abaqus, BMW undertook the challenge to predict the performance of a large car front end BIW made entirely from composites. Low and high speed load cases for both full frontal and offset frontal impact against a rigid barrier were considered. Data from the three crash tests of the full system configurations compared

well against simulation results obtained prior to the crash tests.

The CZone approach to composite impact is based on the principle of applying the forces generated through the fragmentation of the composite at the crushing interfaces to the adjacent finite elements. These forces are transferred back into the rest of the structure away from the crush zone and can potentially instigate non-crushing failure of the composite structure, an important design consideration. The “crush stress” which is assigned to the finite elements is considered as a macroscopic material property and can be measured via laboratory coupon testing.

INTRODUCTION

Worldwide energy consumption is projected to increase by 53% between 2008 and 2035, with the demand for liquid fuels increasing more rapidly in the transportation sector than in any other end-use sector [1]. Motivated also by initiatives to reduce the production of greenhouse gases, there is a clear move to make automobiles and other light vehicles more fuel efficient. Whether conveyed in the U.S. as improved fuel economy or in Europe as reduced tailpipe emissions, the entire automotive industry is moving in the direction of significantly improving fuel efficiency.

There is general recognition in the industry that powertrain innovations alone will not be sufficient to meet the required

targets. Lightweight vehicle design is recognized as an important measure to reduce vehicle weight and gain fuel efficiency. Figure 1 shows that, by at least one estimate, “Light Weighting” ranks third in terms of influence on improving fuel economy and reducing emissions [2].

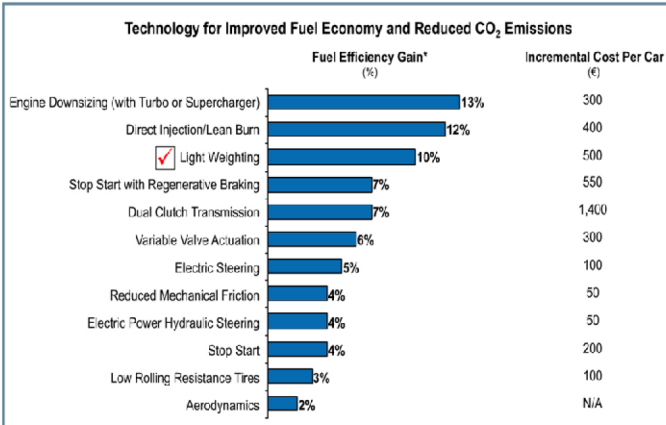


Figure 1. Technologies for improving fuel efficiency.

Lightweight vehicle design enables reversing the weight spiral that has evolved over the past few decades, as vehicles have generally become larger and heavier [3]. A lighter vehicle platform allows subsequent downsizing of the powertrain, cooling unit, fuel tank, brakes, and other systems, thus starting to move down the weight spiral rather than continuing to move upward.

Carbon fiber reinforced polymer (CFRP) materials are expected to play a meaningful role in contributing to lightweight vehicle design in the coming years. Both the military and, more recently, commercial aircraft industries are already incorporating significant carbon fiber content into airplane designs. The automotive racing sector has long employed CFRP materials, not only for their high strength-to-weight and stiffness-to-weight ratios, but also for their high energy absorption capacity to dissipate energy in a crash event.

Crushing of Composite Materials

Figure 2 shows a sequence of images for the dynamic impact of a laminated CFRP plain cone structure. As compared to the buckling and folding deformations common in steel and aluminum structures when subjected to similar loading, the CFRP structure essentially pulverizes into small fragments and other fine debris over the duration of the impact event.

“Crush” is the ability of a material to continuously absorb energy through destruction/disintegration of the composite material. The mechanisms by which this material fragmentation occurs are very complex, involving many micromechanical interactions of the fiber and matrix constituents and their bonded interfaces. When crush occurs, many of these bonds fail, along with individual and collective

fiber buckling and associated sliding friction and accumulation of microscopic debris, all serving to create further debris and absorb further energy as the crush front develops. This essential disintegration of the material when it crushes contributes to the much higher specific energy absorption (SEA) when compared to the buckling and folding mechanisms that typically occur in a comparable steel or aluminum structure. Figure 3 characterizes typical load-displacement response for a CFRP material that is crushing in a stable manner, as the crush front progresses through the structure in a continuous manner.



Figure 2. Dynamic impact loading on a CFRP cone structure.

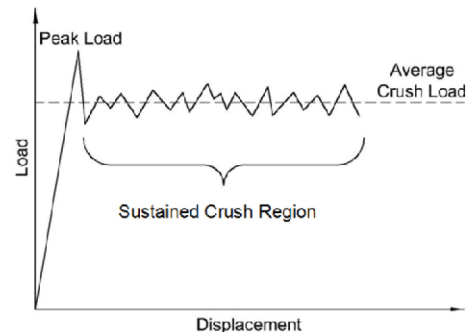


Figure 3. Stable CFRP crushing response.

Not all CFRP materials exhibit stable crushing behavior however, as shown in Figure 4. The response is characterized more by multiple fractures away from the impact region; significant portions of the material are left largely intact, having absorbed only a fraction of the potential energy that may have been absorbed via crushing.



Figure 4. Example of CFRP material exhibiting poor crushing behavior.

Incorporating Composite Crushing in Passive Safety Design Simulation

BMW have placed significant emphasis over several years on “predictiveness” for passive safety design simulation, with the overarching objective to largely eliminate prototype

fabrication and testing [4]. This objective has been achieved recently with the 6 Series Gran Coupe; this model is representative of more conventional steel-dominated vehicle platform construction.

In a vehicle platform which incorporates CFRP structures intended to absorb crash energy via crushing, the capabilities of passive safety design simulation must be extended to account for two important phenomena: 1) simulating the crushing response as it develops during an impact event, and 2) transferring the forces that develop at one or multiple crush fronts to regions away from these crush fronts into the surrounding structures. The latter is particularly important in order to ensure that the CFRP structure is properly designed to not fail prematurely due to a non-crushing failure away from the crush front, and thus negate a substantial portion of the energy absorption duty for which it was intended. [Figure 5](#) shows an example where a CFRP structural member subjected to a 30 degree offset impact fractures in a catastrophic manner before any crushing response can develop.

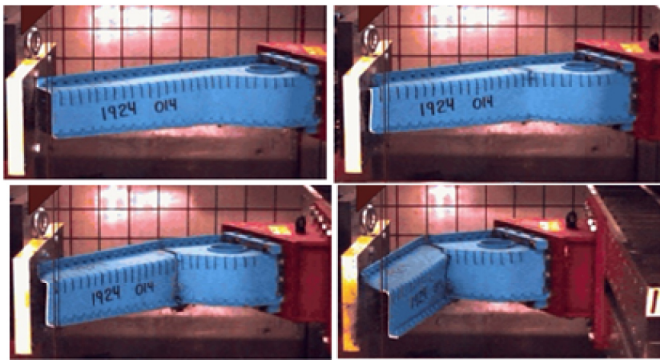


Figure 5. Non-crushing fracture failure away from the intended crush front.

However, robustly simulating the crushing response of CFRP materials in a predictive manner, as well as at reasonable computational cost, has proven difficult, as noted in [5], [6], and [7]. The explicit finite element analysis codes utilize broadly similar composite failure modeling, where, as an element is loaded, the stresses/strains in the individual plies are calculated based on their stiffness. When a ply within a given element is loaded until it reaches its failure condition, for example using the Tsai-Wu failure criterion, the ply is either failed instantly or rapidly degraded to provide a zero stiffness contribution, and for CFRP materials, occurs in the order of 1.0-1.2% strain. This is a traditional failure mode, i.e. cracking of the structure. At every time step these failure calculations are simply repeated. Once all plies in a given element have reached their failure load, the element as a whole is deleted from the model. Failure is a sudden event as a consequence of the force applied to the element, which is in effect a function of its own stiffness [8]. This type of failure criterion achieves reasonably good correlation for ply and

element failure in a bending fracture mode, such as that shown in [Figure 5](#).

However, applying such an approach to simulate crushing failure response generally produces results that do not correlate as well against experimental measurements. While documented more thoroughly in [9], [Figure 6](#) shows a simplified illustration of response for a CFRP column subjected to dynamic axial loading from a rigid impactor. Considering a simplified structure with only unidirectional plies, and using the same methodology as described above, an element is loaded according to its elastic stiffness up to its ultimate compressive failure stress, at which point failure is considered to initiate and the element stiffness is then rapidly degraded. This sequence is repeated as the impactor motion progresses through the length of the column.

As shown in [Figure 6](#), such response contrasts somewhat with what is typically measured experimentally for CFRP materials that exhibit stable crushing behavior. Peak forces in the simulation are somewhat greater than those measured experimentally, while at the same time, the energy absorbed via crushing in the simulation is somewhat less than what is measured.

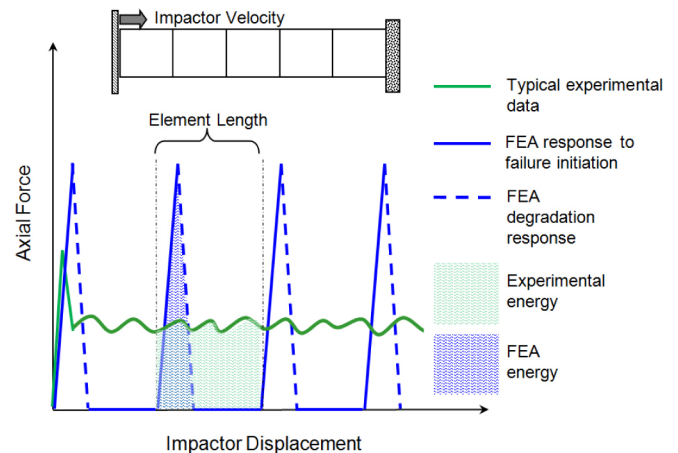


Figure 6. Simplified conventional explicit FEA response for axial crush test.

For the CFRP material used in the Low Speed Energy Absorber structure discussed later in this paper, the documented elastic compressive modulus is 100 GPa, and the compressive failure stress is 621 MPa. However, the experimentally measured stable crush stress for this material is 134.5 MPa. Hence, the simulation generates peak forces (stresses) that are a factor of 4.6 greater than what occur in the physical structure.

According to the simplified conventional failure modeling approach, the energy density absorbed via crushing is approximately (from linear elasticity):

$$U_0^{fail} = \frac{(\sigma_{comp})^2}{2E} = \frac{(621 \times 10^6)^2}{2(100 \times 10^9)} = 1.93 \times 10^6 \frac{\text{J}}{\text{m}^3}$$

However, the measured energy density absorption is essentially the same value as the stable crush stress ($134.5 \times 10^6 \text{ J/m}^3$), a factor of nearly 70 greater than that predicted by simulation.

Filtering can be applied in a post-processing manner to reduce the simulation peak forces and smooth the resulting force-displacement curve. Likewise, numerical parameters can be introduced in the simulation to ensure that only elements at the intended crush front will experience crushing failure. However, with this failure modeling approach applied to crushing response, it's generally not possible to correlate both with the experimentally measured forces and energy absorbed during crushing.

The consequences of generating much larger forces or stresses in the simulation than observed experimentally are potentially severe in terms of accurately predicting the integrity of the surrounding composite structure, away from the crush front. While these large stresses act only over a very short period of time (i.e., the load on the element is increased until it fails instantaneously and no resistance by this element is maintained since the element is then deleted), they are still propagated through the composite structure. In design simulations for complex structures, this can result in an unrealistic prediction of non-crushing failure of the composite structure at distances away from the crush front, and thus compromising a primary objective for such design simulations.

CZone Approach for Composite Crushing

The basis for CZone (short for Crush Zone) recognizes “crush stress” as a distinctive mechanical property of a composite material [10]. Like other mechanical properties, such as yield stress for a metal, it can be measured experimentally. The CZone approach can be considered a phenomenological method in that it does not seek to model any of the micromechanical interactions between fiber and matrix that occur during crushing.

The crush stress property can be obtained through various test methods. The most feasible and cost-effective is crush testing of coupons extracted from flat plaques or sheets of the candidate laminate. The coupons can readily be cut from the flat plaque using a water jet, and have a saw-tooth shape cut into one end in order to induce the initiation of crushing. Crushing is carried out with a specially designed test fixture that can be placed in any suitable loading apparatus, such as a high-rate Instron machine.

Experience has indicated that higher values of crush stress can be obtained for curved sections of a CFRP laminate versus flat sections, and hence it is often desirable to incorporate curved sections into a structural member in order to increase its energy absorbing capacity. This observed difference in crush stress is presumed to be caused by an enhanced suppression of ply delamination just ahead of the moving crush front for curved sections versus flat sections.

The crush stress property for curved sections can be obtained from crushing a suitably fabricated specimen, such as a sinusoid shape. But it can also be obtained using the specially designed test fixture noted above by including three stabilizing pins in the fixture which are intended to restrain the delamination of the flat coupon specimen and hence mimic the curvature effect while still testing coupons extracted from a flat plaque.

CZone technology is available commercially within the Abaqus finite element software suite, namely Abaqus/Explicit, an explicit dynamics solver used across several industries for various applications, including crashworthiness and occupant safety. The integration of CZone within the framework of a commercial finite element software suite thus has the benefit that the wide range of features and functionality already available in the commercial software package can be used in conjunction with the specialized crushing simulation capabilities of CZone. For example, failure models already available to predict the potential for non-crushing failure away from the crush front can be used simultaneously with CZone.

From a usage perspective, CZone works in conjunction with shell elements in Abaqus/Explicit. For those model components to be considered for potential crushing within a given simulation, crush stress properties are entered for those CFRP components similarly as material data and assigned on a shell section (or laminate) basis. The potential for crushing in a particular CFRP component is further defined through contact pair specification(s) between the CFRP component and one or more other components that it may come in contact with during the simulation.

During the course of the simulation, the contact state between the CFRP component and its counterpart(s) in the contact pair specification(s) is continually monitored. When contact forces sufficient to induce crushing are detected, the crush stress properties then dictate the manner in which resisting forces are applied at the crush front. For a given element within the CFRP component undergoing crushing, these resisting forces are applied in a continuous manner as the element passes through the crush front. Once a given element passes completely through the crush front, it is deleted from the simulation. Elements deleted due to crushing produce no residual debris to play any further role in the simulation. However, it is possible that non-crushing failure may produce

fragments that are still active for the remainder of the simulation.

Further discussion concerning CZone usage, as well as examples of comparisons of CZone simulations against experimental data, can be found in [10], [11] and [12].

COMPONENT CRUSHING STUDY

A component crush study was initiated in order to begin to assess the capabilities of the CZone approach, both for predicting the dynamic crushing response, as well as the ability to predict non-crushing failure away from the crush front.

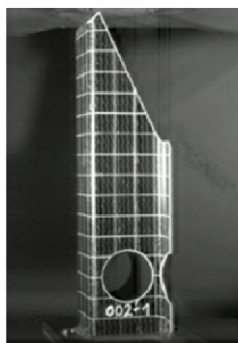


Figure 7. Hat section CFRP component for crushing study.

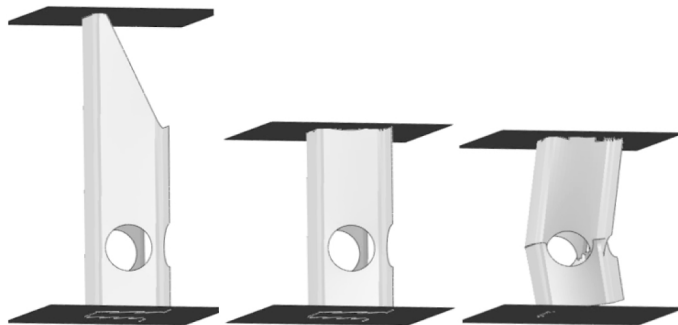
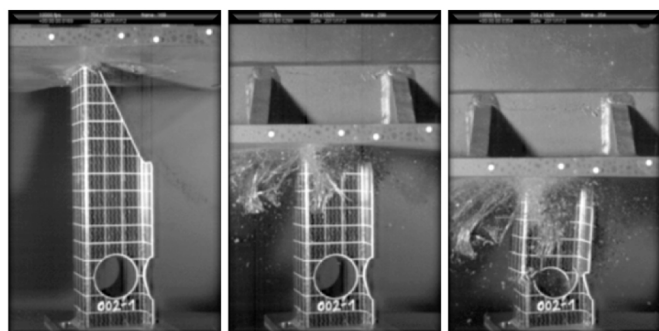


Figure 8. Comparison of component crushing sequence for physical test and simulation.

Figure 7 shows the CFRP component, a hat section profile tapered at one end in order to readily initiate crushing at that location, as well as to provide an increasing resistance as the

crush front moves progressively through the length of the component. In addition, large circular holes were cut on either side of the hat section near the opposite end of the component, along with half-circular cuts in the flanges in the same region. This was done purposely to initiate a non-crushing failure at some point during the impact event and hence test how predictive the corresponding simulation would be for this response.

Figure 8 shows a sequence of images comparing results from the physical test with those from the corresponding simulation, while Figure 9 compares the load-time histories. Results indicate that both the crushing behavior, as well as the initiation of non-crushing failure away from the crush front, are captured well in the simulation. The sudden drop in force that is observed both in the experimental data and simulation results occurs when the component fails catastrophically at the circular cutouts in the component away from the crush front (last frames in Figure 8).

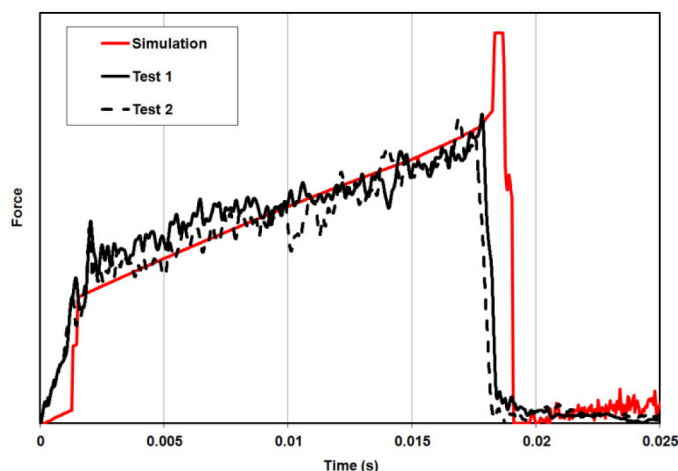


Figure 9. Comparison of force-time response for component crushing test.

VEHICLE PROJECT

Over the past few years, passive safety design simulation processes at BMW have been extended to incorporate the unique features of the i3 vehicle platform, namely its passenger cell constructed entirely of CFRP material. However, the i3 presently does not rely on CFRP material for energy absorbing structural members, instead utilizing more conventional aluminum construction for its bumper system and longitudinal members.

Encouraging results from the CFRP component crushing study motivated a next step, namely to investigate the “predictiveness” for simulating composite crushing and crashworthiness at the full vehicle or system level. One requirement in order to incorporate CFRP materials into primary structures is to be able to carry out passive safety design simulation with the same level of accuracy and

robustness as is presently achieved for conventional metallic vehicle platforms. It must be feasible to achieve passive safety performance targets largely through design simulation, while minimizing the amount of prototype fabrication and testing.

Hence a project was formulated to assess the viability of current passive safety design simulation capabilities at the system level. A current series production front end BIW was chosen as the basis for the investigation. [Figure 10](#) shows the present aluminum front end structure which was to be redesigned with CFRP components.

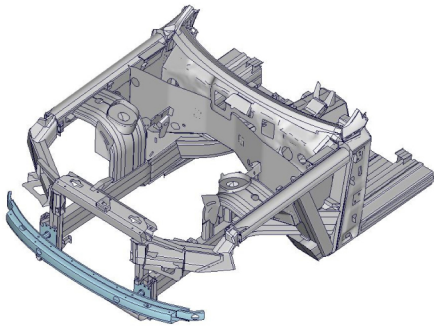


Figure 10. Aluminum front end structure to be redesigned with CFRP components.

Objectives

The overall objective was to replace the present aluminum BIW front end structure with one constructed entirely of CFRP components, and to subsequently meet passive safety performance targets. Ambitious objectives, along with some corresponding constraints, were established at the outset in order to best assess present design simulation capabilities, as well as to identify areas where further investigation and improvement would be needed.

1. Design iterations were to be carried out exclusively through the use of simulation, prior to physical testing. Physical test data were not to be utilized in order to “tune” the simulation models to match the test data.
2. Passive safety tests to be carried out included low and high speed load cases for both full frontal and offset frontal impact against a rigid barrier.
3. The CFRP-intensive front end redesign was to be carried out within the present BIW geometry package. In particular, the present vehicle engine, cooling system, and tire package represented geometrical constraints to be accommodated during the redesign.
4. Only crush stress properties obtained from coupon testing were to be utilized for the design simulations.
5. Other design criteria for the present aluminum BIW front end structure, including static strength and NVH performance, had to be achieved also in the CFRP redesign.

CFRP Structure Development

[Figure 11](#) shows the overall configuration of the CFRP front end redesign. The strategy employed to objectively compare simulation results against subsequent physical test data involved mounting the front end structure to a steel frame representing the rear part of the vehicle chassis. This provided a stable platform to support the front end structure. The frame allowed for the mass of the impacting “vehicle” to be adjusted as needed, and it also carried the data acquisition equipment. The physical crash tests were then to be carried out by accelerating the front end/frame assembly representing the vehicle to the prescribed test speed. Upon subsequent impact with the rigid barrier, the front end/frame assembly could then move freely in yaw and pitch.

Simulations of this test configuration with an aluminum front end structure were carried out in advance, and results indicated nearly the same performance as for the actual full vehicle. Hence the test configuration was judged to be valid for assessing the CFRP redesign of the front end structure.

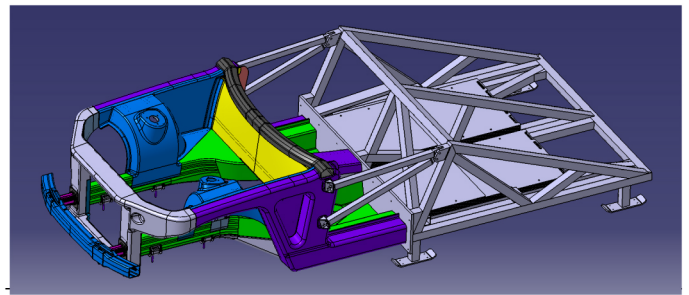


Figure 11. CFRP front end and steel frame assembly.

As required within the overall project objectives, the CFRP structure development was simulation-driven. Numerous component models and corresponding simulations were executed to establish and validate the fundamental design concepts for section sizes and crush lengths to meet the passive safety requirements. The design process subsequently progressed through a series of subassembly models, leading eventually to full system level models and simulations.

The primary focus areas for development of the CFRP redesign were the Low Speed Energy Absorber (LSEA) and the longitudinal member ([Figure 12](#)). In the low speed crash tests, the LSEA is intended to dissipate the crash energy while leaving the longitudinal member undamaged. In the high speed tests, the two structures are intended to crush in sequence, with crushing of the LSEA leading to subsequent crushing of the longitudinal member. Once these basic designs were established, the remaining structure connecting these elements to the passenger survival cell was developed, incorporating features for the under-bonnet and suspension packaging.

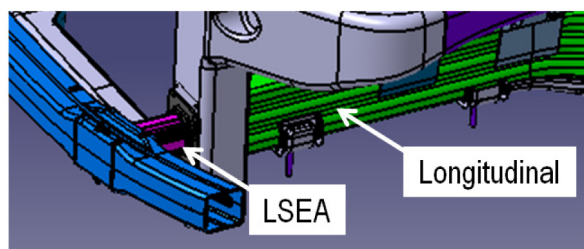


Figure 12. LSEA and longitudinal member.

Low Speed AZT Requirements

The AZT test is not legislative but is an insurance rating test to determine the cost of reparability in low speed impacts of 16 km/hr. The vehicle is subjected to a 40% overlap rigid barrier angled at 10 degrees at a vehicle weight of 2600 kg. In order to obtain a high rating in the test, after the impact the vehicle is required to be drivable to a repair center and the cost of damage is assessed. Ideally, the structures damaged under this test will be simply unbolted and replacements installed.

LSEA Development

Geometric packaging constraints imposed primarily by the body outer and bumper system in the current production vehicle limited the available crush distance for the LSEA before the bumper structure contacts the radiator surround. One key benefit of CFRP energy absorbing structures is that they can be designed to have a nearly square wave crushing response to impact, and thereby be efficient at dissipating energy with a minimum peak force, a characteristic which is very difficult to achieve with metal structures. The package space available for crush in the bumper and LSEA before damage was sustained to the primary body structure was 110 mm in total. Along with the required energy level to be absorbed in the offset AZT test, this established the average crush force to be achieved in the LSEA. This force level also set the design objective for the crush forces to be generated in the primary high speed energy absorbing member, the longitudinal.

A preliminary LSEA section was designed based on a two-part "tube" component with bonded flanges that was suitable for high volume manufacture, able to locate within the present bumper system, and capable of generating the necessary crush forces, while also capable of withstanding the lateral loadings due to the angled impact on the rigid barrier. [Figure 13](#) shows the LSEA, along with the LSEAs in the bumper assembly.

With composite tubes, the initiation of stabilized crushing is an important design aspect - if left as a square cut the front end of the tube will initially fail through material compression. The inertial effect will amplify the stresses at the front of the section, however the inertial effect is not high and, due also to imperfections in the materials throughout the

section, an undesirable non-crushing failure could develop away from the intended crush initiation at the front end. In order to develop the design to robustly initiate crushing at the front, the LSEA is tapered away from the front centre vertical fixing. This also has the effect of preventing the bumper leveraging on an edge of the LSEA due to the 10 degree impactor angle for the offset frontal impact tests. A further technique often employed is to put a chamfer on the edge of the tube to reduce the initial force and to initiate a stable crush front. However, this process is relatively difficult to achieve in production, and so a crenellated front edge was employed, as can be seen in [Figure 13](#). The small axial cuts act as an artificial crush front and therefore introduce initial crush forces at a level that the section properties can continue to sustain. Once crushing has initiated at the front of the LSEA, compressive stresses further back in the component are at levels which do not exceed 27% of the allowable compressive stress.

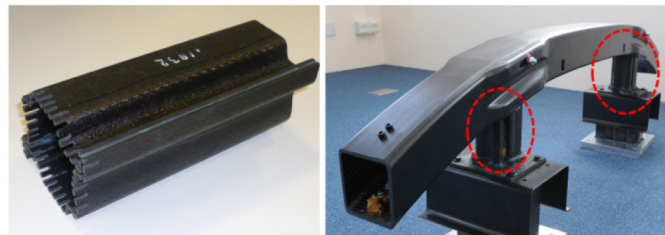


Figure 13. LSEA structure (left) and highlighted in the bumper assembly (right).

The subassembly and full vehicle simulations identified a recurring issue in the design which initiated premature collapse of the LSEA structure. This was caused by the sides of the bumper structure impacting in an out-of-plane direction with the LSEA side surfaces. This caused local damage and, as a result of the consistently elevated stress levels in the LSEA due to compressive loading, caused catastrophic collapse.

Subsequent modifications were undertaken to alleviate the chances for this type of premature failure, and the design was released for manufacture and components built. Unfortunately, the final simulation predictions prior to the physical test indicated a recurrence of the premature collapse of the LSEA. Many of the interim design modifications did not demonstrate this failure and, on closer inspection of the analysis results, it was shown that a piece of uncrushed debris from the back of the bumper impacts the highly compressively loaded side face of the bumper. With test components already produced, the decision was taken to proceed with the test.

AZT Test Results

The full vehicle front end assembly was tested with the full composite bumper system in place according to the AZT test specifications. The crush length within the LSEA was very

close to the simulation prediction, at 107 mm measured after the event. [Figure 14](#) shows the CFRP front end structure following the AZT test. The bumper beam remained connected to the front of the body structure through the compaction of the debris in the engineered voids between the LSEA and the internal surfaces of the bumper. Tools were required to lever off the bumper beam from the LSEA stub, confirming that the vehicle would have been in a position to continue to a repair center without the need for recovery.

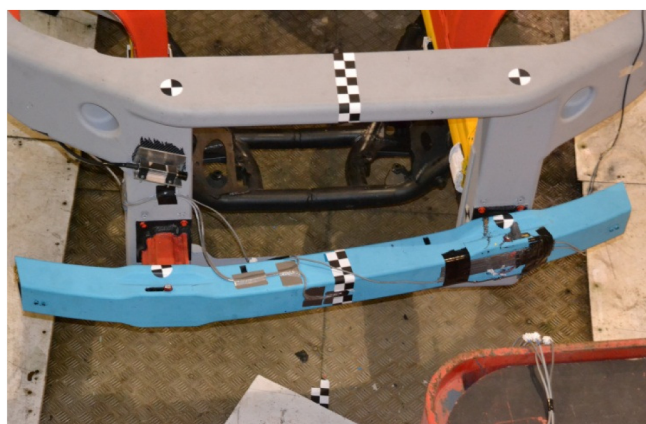


Figure 14. CFRP front end structure following AZT test.

[Figure 15](#) shows a detailed view of the LSEA and surrounding region both before and after the test.

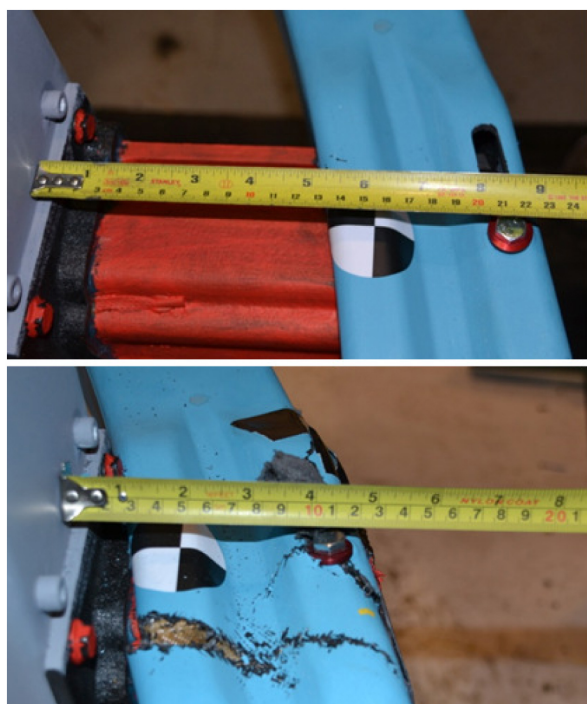


Figure 15. LSEA and surrounding region before and after AZT test.

[Figure 16](#) shows a comparison of acceleration for simulation prediction versus physical test result. Correlation between

simulation results and test data, while reasonably good, is not as strong as for the earlier component test ([Figure 9](#)). In the earlier component test, the primary variability was in the tested component itself - no other components or connections were present. The two sets of experimental data confirmed the repeatability of the test and the low variability. In the AZT test, while crushing of the LSEA structure is the primary subject of investigation, both the physical test setup and the corresponding system level model are far more complex than the previous component test, with numerous components and subassemblies and associated connections. These likely introduce greater variability into the test which leads to less strong correlation between simulation results and experiment data than for the earlier component test.

Also, [Figure 16](#) represents the acceleration as a function of vehicle longitudinal displacement, which is computed as the double integral of acceleration for the physical test. The accelerometers were mounted in the rear of the tested assembly, and therefore the computed displacements include the additional strain developed in the region from behind the LSEA flange up to the accelerometer location, and which is elastically restored after impact.

The premature failure of the LSEA in the final simulation results for the AZT noted earlier is evident in the drop-off to zero acceleration at about 120 mm in [Figure 16](#).

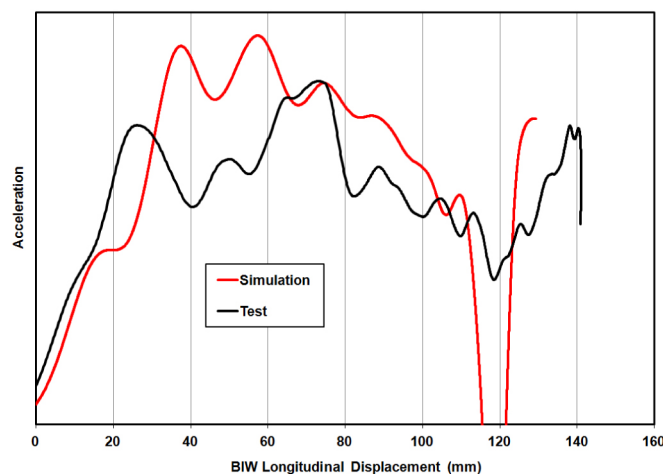


Figure 16. Comparison of acceleration histories for AZT load case.

High Speed Load Cases

The frontal high speed load cases involved both full and 40% overlap tests at 56 km/hr against a rigid barrier with a vehicle mass of 931 kg. In addition to acceleration/force requirements, no intrusions into the passenger cell were to occur. An additional requirement specified for this project was that sufficient crushing would be achieved to move the subframe rearward by at least 120 mm.

Longitudinal Development

Following the successful simulation-driven development of the LSEA structures, the specification and requirements of the high speed energy absorbers (longitudinals) became more established, in particular the threshold at which crushing in the front of the longitudinals is initiated. The sustained crush force in the LSEAs has a degree of variability in the order of $\pm 10\%$ when considered over the duration of the AZT test.

After 107 mm of crushing is reached, the forces necessary to continue further crushing in the LSEA are intentionally increased through additional layers of material for the last 30 mm ahead of the support flange. As the whole of the LSEA is consumed, the bumper attachment bolt collides with the thicker rear flange of the LSEA, and the forces increase over a short distance. This spike in the forces is required to initiate crushing in the front of the longitudinal on the rear of the plate that connects the two structures together.

The commencement of crush in the longitudinal posed significant challenges to the development of a robust and reliable solution to address the dual needs of providing sufficiently high LSEA crush forces, while also resisting crushing in the longitudinals for a low speed load case, and maintaining structural integrity in the surrounding CFRP structure for both low speed and high speed impact events. Figure 17 shows how the design crush forces for the LSEA and longitudinal are relatively close in magnitude, due somewhat to the geometric packaging constraints imposed from the current production vehicle for this project.

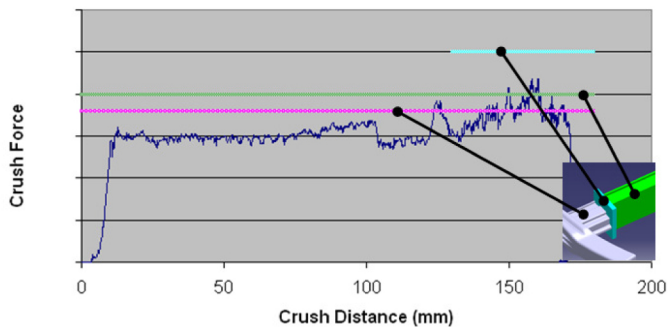


Figure 17. Design crush forces in LSEA and longitudinal.

To initiate crushing, a plane-fronted longitudinal will require a relatively large force spike. Due to the short duration of this force, it would not be considered too high for occupant safety, but such a force level would transmit forces to the surrounding CFRP structure around the passenger safety cell that would mandate extensive reinforcement around the passenger safety cell. Furthermore, the longitudinal itself cannot be overly reinforced due to the consequence of elevating the crush forces to levels which would induce occupant injury. An initiation force that is too high would also increase the risk of breaking off large sections at the

front of the longitudinal which would therefore no longer be able to crush and absorb the impact energy.

Simulation was utilized to drive the investigation to find the most viable forced-based crush initiation in the longitudinal. The final scheme utilized a series of holes at the interface to the longitudinal and the plate supporting the back of the LSEA. The size and location of the holes is essential for insuring the initiation load is above the variability in the LSEA crush loads, but also below the loads at which failure will occur elsewhere in the CFRP support structure.

Figure 18 shows three crush initiator schemes that were analyzed to determine the force levels required to cause compressive failure across the front section of the longitudinal and hence start the crushing mode.

1. The left figure shows a scheme that creates an initiation force in excess of the failure load at the rear of the longitudinal structure where stress concentrations occur at a section change approximately 300mm in front of the lower firewall.
2. The middle figure has an initiation load near the peak levels that could be expected in the LSEA crush and at the end of the AZT test. As a result, while not a threat to the passenger safety cell, these suppressed initiation levels could lead to premature crush initiation of the longitudinal in a low speed impact, leading to greater vehicle damage in what would be expected to be a more easily repairable accident event.
3. The right figure shows a configuration of initiation holes where the load levels generated in the interface before crush initiated in the front of the longitudinal were safely in excess of the peak loads generated in the LSEA, and equally safely below the loads which would cause premature failure in the surrounding CFRP support structure. This configuration was predicted from simulation to initiate crushing in the longitudinal at an appropriate level of force.

As with the LSEA, simulation provided the means to design the longitudinal to maximize the energy absorbed in the available crush distance without inducing force levels that would lead to instability in the moving crush front or compromise the integrity of the passenger safety cell.

While the design intent is to absorb crash energy through crushing both in the LSEAs and longitudinals, the design process must consider the possibility for non-crushing failure, such as fracture due to high bending loads. Figure 5 previously illustrated the potential negative consequences when the latter occurs. The simulation methodology employed throughout the project simultaneously invokes CZone in the expected crush regions, along with the Tsai-Wu failure criteria [11] throughout the entire CFRP front end structure. The combination of the two enables a progression

of design iterations that can most efficiently be carried out to achieve the required design objectives.

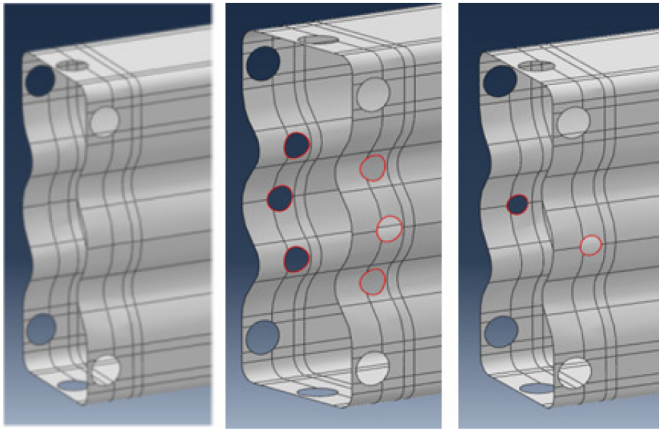


Figure 18. Longitudinal crush initiator schemes considered.

The prediction of crush initiation, for instance at the front of the longitudinal, is not specifically a crush simulation issue. Tsai-Wu was employed here also to predict the CFRP material failure in this region which would then initiate subsequent crushing in the longitudinal.

High Speed Full Overlap Test Results

Having utilized simulation to develop the initiator scheme for the front of the longitudinal, subsequent simulation of the full overlap load case for the full vehicle was the most straightforward of the high speed load cases to consider. The LSEAs absorb 25% of the energy and then stable crush is initiated in the longitudinal. As noted earlier, a key objective of the project was to demonstrate that it was possible to crush the longitudinal for at least 120 mm past where the subframe is contacted by the barrier. The simulations predicted that the safety cell would withstand the impact with no damage and that the average deceleration levels were very close to those with the present aluminum structure.

The physical testing of the front end identified a vulnerability which was not identified by the analysis, but was also not consistent between the left and right side of the vehicle. The right LSEA structure was partially crushed at a point when the aluminum plate in front of the initiators in the right longitudinal failed and crush commenced prematurely in that longitudinal. In the test, crush continued as the LSEA backing flange was forced down the internal section of the longitudinal. However, significant portions of the longitudinal side faces were detached and therefore no longer available for energy absorption. This premature failure sequence did not occur on the left side.

Despite this premature failure, the structure absorbed energy and continued to crush past the 120 mm minimum distance of the subframe moving rearward. The passenger safety cell

remained undamaged, and the force levels did not rise to unsustainable levels. Although there is an obvious discrepancy in the observed test performance between the left and right side on what is a symmetrical structure, the robustness of the prediction of crush initiation is called into question. The initiation is handled by the Tsai-Wu failure criterion presently within the simulation methodology and is an area which needs further investigation and development.

Figure 19 shows a sequence of images comparing results from the physical test and the simulation carried out prior to the physical test. Accumulation of debris from the LSEAs and longitudinals due to crushing begins to obscure the visibility of the longitudinals as the physical test progresses.

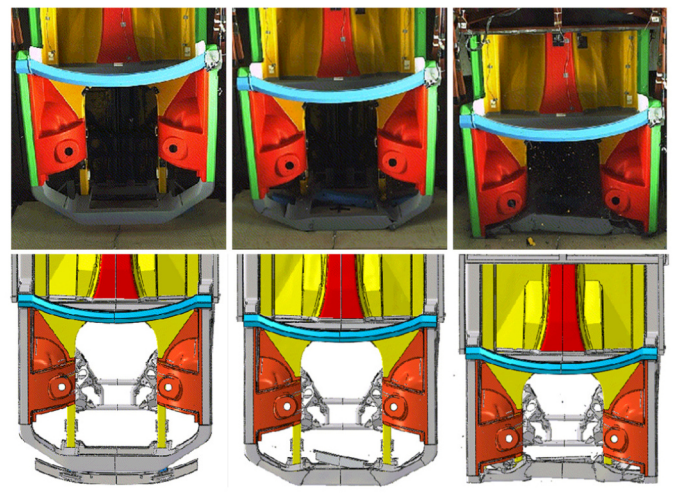


Figure 19. Image sequence for high speed full overlap load case for physical test (top) and simulation (bottom).

Figure 20 shows a comparison of acceleration histories for both simulation and physical test for the high speed full overlap load case. The effect of the failure of the aluminum plate between the right LSEA and longitudinal which results in the premature partial failure of the right longitudinal is evident in the decrease in deceleration that begins at approximately 80 mm displacement, and the subsequent increase that begins at approximately 140 mm displacement.

The premature failure of the aluminum plate on one side of the vehicle is not desirable, and furthermore would not give an adequate surface for the longitudinal member to subsequently crush against in a production structure. While unexpected, this result is leading to the development of simulation protocols to include the potential for failure in all metallic structures that are intended as impact surfaces for the crushing composite. In situations where failure of the crushing surface is predicted, the design will be modified to alleviate such failure.

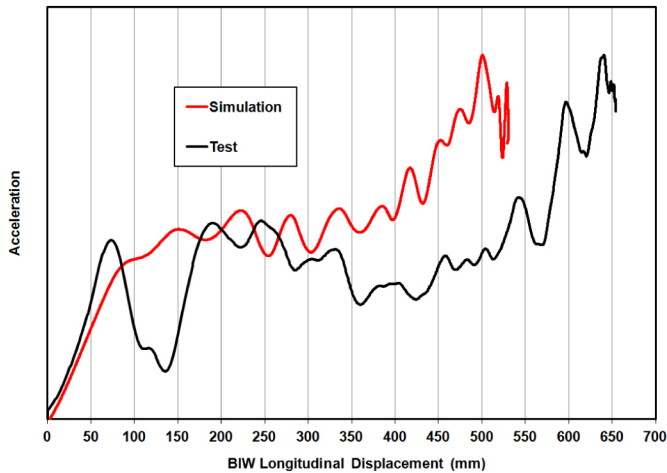


Figure 20. Comparison of acceleration histories for high speed full overlap load case.

High Speed Offset Load Case and Test Results

For the 56 km/hr 40% offset load case, design simulations at the full vehicle level showed a successful consumption of the full LSEA structure and initiation of crush at the front of the longitudinal. However, as the impact event progresses, rotation of the entire vehicle begins to build up due to the offset nature of loading conditions in the test, and the impacted longitudinal is observed to “wipe” across the face of the barrier. This wipe effect induces considerable bending forces on the longitudinal and, because of the fragmented crush front, the side faces become independent faces and are torn away from the upper and lower horizontal faces. As the crush continues in the upper and lower surfaces, the sides bend further and cracks form at the corners. They eventually cease to crush and break away from the upper and lower faces, leaving them unstable, and collapse soon follows. This resulting gap in the longitudinal provides no resistance to the advancing vehicle until a new crush front develops between the barrier and remaining portion of the longitudinal, and energy absorption via crushing resumes. The wipe effect then develops again and the same sequence is repeated. Figure 21 shows a schematic of the wipe effect between the longitudinal and barrier.

It was clear from these simulation results that the anticipated crush performance was not being realized, and the efficiency was reduced by the quantity of the uncrushed sections of the longitudinal that fractured and broke away. An effort was undertaken to develop corrective action to address the wipe effect and its consequences. Simulation played a central role in developing a clear understanding of the wipe effect, as well as in designing the modifications in the longitudinal to mitigate the wipe effect and maximize the crushing of the longitudinal. Figure 22 shows a comparison of crush forces predicted from simulation for a longitudinal in its original design as well as subsequently modified with the “anti-wipe” features. The consequences of the wipe effect in the original

design are very apparent as the crush force drops rapidly to zero when portions of the longitudinal fracture and break away. While with the anti-wipe features in place, a reasonable crushing force is maintained over the duration of the event.

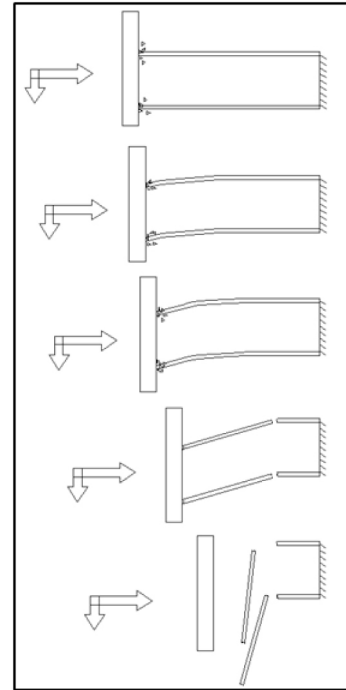


Figure 21. “Wipe” effect interaction between longitudinal and barrier in offset loading condition.

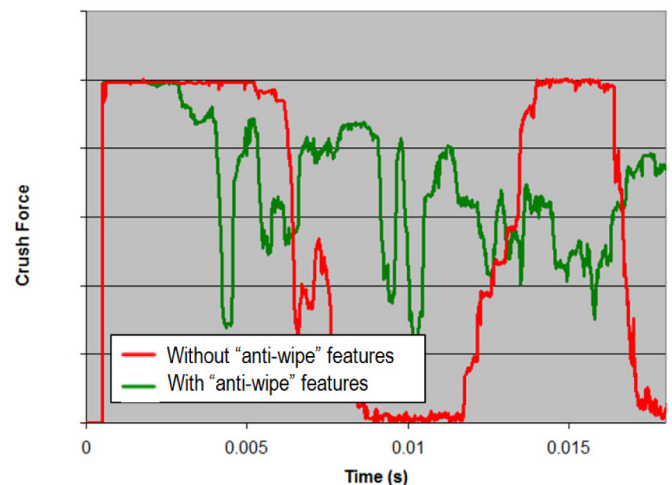


Figure 22. Comparison of longitudinal crush force histories with and without “anti-wipe” features in place.

Having developed the local details of the longitudinal to behave well in the high speed offset loading condition, simulation was further utilized to confirm that the targeted performance level of the full vehicle for the high speed offset load case was also being achieved.

The corresponding physical test for the high speed offset load case was then carried out for the full vehicle. The global results were good, with no failures behind the progressive crush fronts in the LSEA and longitudinal. Crush distances were comparable to the simulation predictions, and full integrity of an intact passenger safety cell was maintained. [Figure 23](#) shows a sequence of images comparing results from the full vehicle physical test and the simulation carried out prior. It is clear from both the test and simulation results that only the right LSEA and longitudinal are absorbing impact energy via crushing. [Figure 24](#) shows a comparison of acceleration histories for both simulation and physical test for the high speed 40% overlap load case.

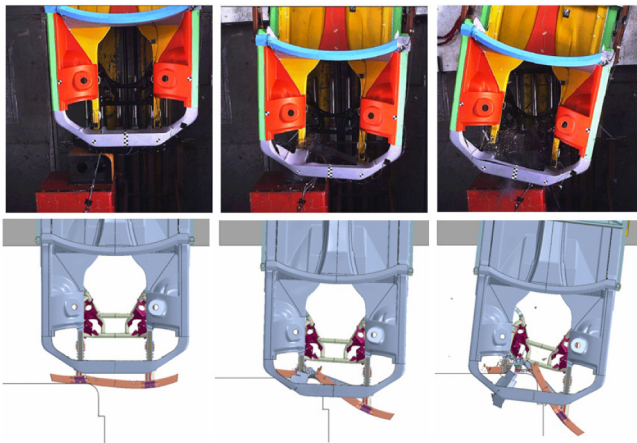


Figure 23. Image sequence for high speed 40% overlap load case for physical test (top) and simulation (bottom).

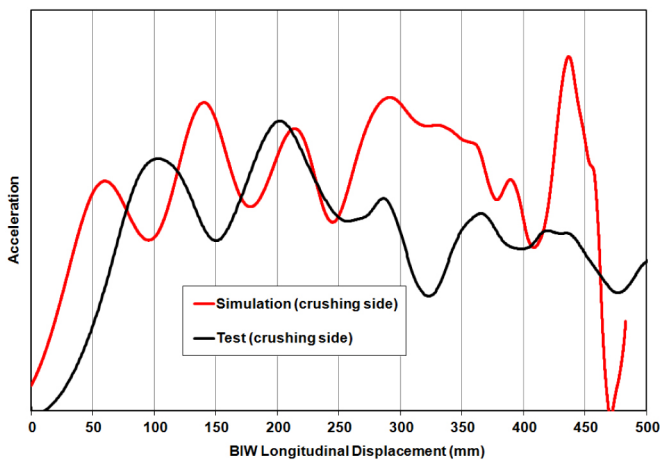


Figure 24. Comparison of acceleration histories for high speed 40% overlap load case.

SUMMARY/CONCLUSIONS

A project utilizing a current series production car as the subject vehicle was established to objectively assess the viability of current passive safety design simulation capabilities at the system level for integrating CFRP components as primary structural members. A simulation-

driven approach was mandated, with simulations required to predict physical test performance, from the component level up through the system level. Material properties utilized in the simulations were based entirely on measured coupon data. In addition, there was no adjustment of simulation parameters allowed following the gathering of data from the corresponding physical tests of components, subsystems, and full "vehicle".

The project was made more challenging by the additional requirement to adhere to the full packaging limitations of the subject vehicle under hood, including integration of the front suspension geometry hardware, subframe, and cooling package. In the normal course of vehicle development, the material strategy will heavily influence the structural architecture, and mass savings would have associated package relaxations, and more specifically, load levels would be reduced proportionally. However, it was accepted that this project was to challenge and understand the limitations of the simulation-driven approach, and not a demonstration of good composite design. Even though the resulting CFRP front end structure is not an optimized composite design, and in some ways could be classified as a black metal structural design, for the purpose of simulation the challenge to produce good comparison with physical test was still valid.

Notwithstanding these additional constraints, the CFRP materials deployed in the redesign of the series production front end BIW proved that composites can effectively absorb the energy of a high speed collision for full size vehicles, while reducing vehicle mass substantially. For this project, mass of the full front end structure was reduced by 45% in moving from aluminum to CFRP construction.

The CZone approach within Abaqus was effective at addressing simulation of the crushing behavior and thereby predicting the corresponding section forces due to crushing. This enabled the detailed design of the component lay-ups and other features designed to ensure a crashworthy structure. This new methodology will form the basis for further development of CFRP BIW structures for passive safety applications within BMW.

There were a number of aspects of the simulations which have been identified as potential areas for improvement or more detailed understanding. Projects are in progress to scrutinize with more detail the initiation and development of failures away from the crush front, particularly those that are needed to initiate crushing. The manufacture of components with enhanced repeatability will allow for a more precise understanding of the predictive performance of the established failure models and will also involve the further development of some of BMW's own failure modeling capability using Abaqus in conjunction with CZone.

The primary hindrance to full deployment in the design process is the computational speed. While the stable time increment for CFRP structures will generally be lower than for an equivalent metallic structure, a number of areas have been identified for improving the computational performance. These include improved parallelization across a greater number of processors and potential subcycling for local finely meshed domains.

The performance of the front end structures showed the capability of meeting the structural requirements at significantly reduced mass. In particular, the bumper subsystem demonstrated an enhanced performance over the solution in the current vehicle.

REFERENCES

1. Energy Information Administration, International Energy Outlook 2011, Report No. DOE/EIA-0484(2011), September 2011.
2. Russo, B., "The Role of Light Weight Materials in China's EV Ecosystem," AutoPlastCON 2012, Shanghai, China, February 2012.
3. Trautwein, T., Henn, S., and Rother, K., "Weight Spiral: Adjusting Lever in Vehicle Engineering," ATZ Worldwide, Vol. 113-05, May 2011.
4. Lescheticky, J., Hooputra, H., and Ruckdeschel, D., "Predictive Crashworthiness Simulation in a Virtual Design Process Without Hardware Testing," 2010 SIMULIA Customer Conference, Providence, RI, USA, May 2010.
5. Deleo, F., and Feraboli, P., "Crashworthiness Energy Absorption of Carbon Fiber Composites: Experiment and Simulation," SPE ACCE 2011, Troy, MI, USA, September 2011.
6. Pinho, S., Iannucci, L. and Robinson, P., "Physically-Based Failure Models and Criteria for Laminated Fiber-Reinforced Composites. Part II: FE Implementation," *Composites Part A: Applied Science and Manufacturing*, Vol. 37, No. 5, pp 766-777, 2006.
7. Brecher, A., Brewer, J., Summers, S., and Patel, S., "Characterizing and Enhancing the Safety of Future Plastic and Composite Intensive Vehicles (PCIVs)." 21st International Conference on the Enhanced Safety of Vehicles, Stuttgart, Germany, June 2009.

8. Caliskan, A. "Axial & Lateral Impact Prediction of Composite Structures Using Explicit Finite Element Analysis," ASME International Mechanical Engineering Congress & Exposition, New Orleans, LA, USA, November 2002.
9. Barnes, G., Coles, I., Roberts, R., Adams, D., and Garner, D., "Crash Safety Assurance Strategies for Future Plastic and Composite Intensive Vehicles (PCIVs)," Final Report DOT-VNTSC-NHTSA-10-01, June 2010.
10. Nixon, S., and Barnes, G., "Effective Crushing Simulation for Composite Structures," ICCM-17, Edinburgh, UK, July 2009.
11. CZone for Abaqus User's Manual 2.4, Dassault Systemes Simulia Corp, Providence, RI, USA, 2012.
12. Barnes, G., "Engenuity Dynamic RR2 Simulations," 59th CMH-17 Meeting Proceedings, Boston, MA, USA, August 2012.
13. Tsai, S.W. and Wu, E.M., "A general theory of strength for anisotropic materials. *Journal of Composite Materials*, Vol. 5, pp. 58-80, 1971.

CONTACT INFORMATION

Juergen Lescheticky
Juergen.Lescheticky@bmw.de

Graham Barnes
GBarnes@engenuity.net

Marc Schrank
Marc.Schrank@3ds.com

The Engineering Meetings Board has approved this paper for publication. It has successfully completed SAE's peer review process under the supervision of the session organizer. This process requires a minimum of three (3) reviews by industry experts.

All rights reserved. No part of this publication may be reproduced, stored in a retrieval system, or transmitted, in any form or by any means, electronic, mechanical, photocopying, recording, or otherwise, without the prior written permission of SAE.

ISSN 0148-7191

Positions and opinions advanced in this paper are those of the author(s) and not necessarily those of SAE. The author is solely responsible for the content of the paper.

SAE Customer Service:
Tel: 877-606-7323 (inside USA and Canada)
Tel: 724-776-4970 (outside USA)
Fax: 724-776-0790
Email: CustomerService@sae.org
SAE Web Address: <http://www.sae.org>
Printed in USA